BIOCHEMISTRY
including biophysical chemistry & molecular biology

Article

pubs.acs.org/biochemistry

Characterizing Substrate Selectivity of Ubiquitin C-Terminal Hydrolase-L3 Using Engineered α-Linked Ubiquitin Substrates

Mario F. Navarro,[§] Lisa Carmody,[‡] Octavio Romo-Fewell,[†] Melissa E. Lokensgard,[†] and John J. Love*[,†]

[†]Department of Chemistry and Biochemistry, San Diego State University, 5500 Campanile Drive, San Diego, California 92182-1030, United States

[§]Sanford-Burnham Medical Research Institute, 10901 North Torrey Pines Road, La Jolla, California 92037, United States

[‡]Sorrento Therapeutics, 6042 Cornerstone Court West, Suite B, San Diego, California 92122, United States

Supporting Information

ABSTRACT: The ubiquitin-proteasome system (UPS) is highly complex and entails the concerted actions of many enzymes that function to ubiquitinate proteins targeted to the proteasome as well as enzymes that remove and recycle ubiquitin for additional rounds of proteolysis. Ubiquitin C-terminal hydrolase-L3 (UCH-L3) is a human cytosolic deubiquitinase whose precise biological function is not known. It is believed to hydrolyze small peptides or chemical adducts from the C-terminus of ubiquitin that may be remnant from proteasomal processing. In addition, UCH-L3 is a highly effective biotechnological tool that is used to produce small or unstable peptides/proteins recalcitrant to production in *Escherichia coli* expression systems. Previous research, which explored the substrate selectivity of UCH-L3, demonstrated a substrate size limitation for proteins/peptides expressed as α-linked C-terminal fusions to ubiquitin and also suggested that an additional substrate property may affect UCH-L3 hydrolysis [Larsen, C. N. et al. (1998) *Biochemistry 37*, 3358−3368]. Using a series of engineered protein substrates, which are similar in size yet differ in secondary structure, we demonstrate that thermal stability is a key factor that significantly affects UCH-L3 hydrolysis. In addition, we show that the thermal stabilities of the engineered substrates are not altered by fusion to ubiquitin and offer a possible mechanism as to how ubiquitin affects the structural and unfolding properties of natural in vivo targets.

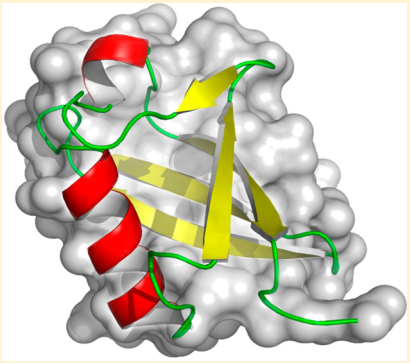

Ubiquitin's name continues to prove appropriate as the number of cellular processes that utilize ubiquitination continue to be discovered and entail essential regulatory events such as endocytosis, transcriptional regulation, enzyme regulation, and protein degradation by way of the ubiquitin proteasome system (UPS).[1−6] Its key role in these processes necessitates a variety of both covalent and noncovalent interactions with a host of other proteins. Early on it was discovered that the sequential action of activating (E1), conjugating (E2), and ligase (E3) enzymes results in the covalent attachment of ubiquitin through its C-terminus to the ε-NH_2 group of a lysine residue on target proteins.[7] Depending on the targeted function, or cellular destination, this is often followed by the condensation of more ubiquitin monomers to the initial ubiquitin moiety to form one or more poly-ubiquitin chains. This simplified description belies the more complex nature of ubiquitination and the many facets of associated biological roles. The functional diversity of ubiquitination is evidenced by the degree of ubiquitination (either mono, poly, or multiple-mono ubiquitination), the particular lysine residue of ubiquitin that is used as the starting point for extension (there are seven lysine residues in ubiquitin), the position and type of residue on the target protein to which ubiquitin is attached (ε-NH_2 group of an internal lysine or α-NH_2 group of the N-terminal residue), and the type of amino acid to which ubiquitin is initially conjugated (e.g., lysine, threonine, cysteine, or serine).[3] Ubiquitin linked through Lys48- and Lys63- have been the most studied to date, but more recently alternative linkages, such as N-terminal Met1-peptide linkages to target proteins, are gaining more attention and provide yet additional complexity to this already multifaceted system.[8−10]

Ubiquitin has been the subject of numerous biophysical and protein engineering studies; however, parallel analysis of ubiquitinated proteins, or ubiquitin polymers, has been limited due to greater complexity associated with systems that specifically produce such complexes.[11,12] In an attempt to gain insight into how ubiquitination affects the biophysical properties of target proteins, one group utilized an in silico approach to study differently ubiquitinated variants of three target proteins.[13] Analysis of mono-ubiquitinated as well as Lys48- and Lys63-linked tetra-ubiquitinated proteins suggests that ubiquitin serves not only as a recognition tag but also may induce or assist protein unfolding and thus possibly enhance degradation through the UPS.[13]

As protocols to obtain different ubiquitin polymers became available, structural information has revealed that linear Lys48-

Received: May 23, 2014
Revised: November 3, 2014
Published: November 4, 2014

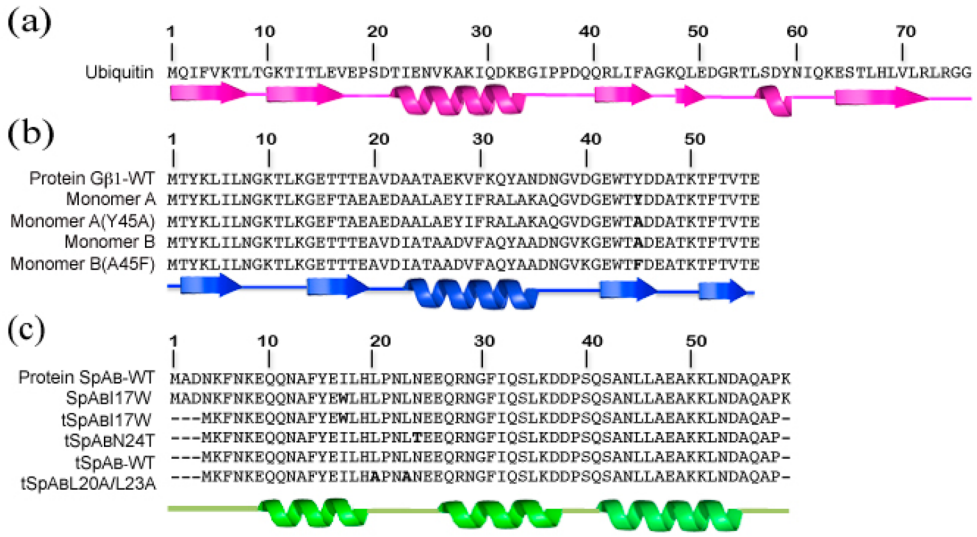

Figure 1. Amino acid sequences for ubiquitin (a), Gβ1-WT and variants (b), and SpA_B-WT and variants (c). The secondary structure for each group of proteins is illustrated with a ribbon diagram below each set of sequences. Relevant mutations of interest are shown in bold face (PDB accession codes: 1UBQ, 2GB1 and 1BDC respectively).

and Lys63-linked ubiquitin possess distinct topological properties.[14−16] Lys48-linked ubiquitin adopts a compact structure, and the ubiquitin moieties interact with each other, whereas linear and Lys63-linked ubiquitin has a more relaxed conformation, and no appreciable interaction is observed between the ubiquitin units.[14,17,18] These findings begin to shed light on the biophysical effects that different types of ubiquitin ligations have on the target proteins as several ubiquitin-binding domains (UBDs) were computationally shown to interact with different poly-ubiquitin variants in a variety of ways. More recently analysis of 482 in vivo ubiquitinated substrates revealed that overall ubiquitination sites tend to be located in structured regions, unlike phosphorylation sites, which tend to be in disordered regions.[19] For a subset of substrates targeted for proteasomal degradation, there appears to be a bias for the ubiquitination site to be located in disordered regions. However, there are still many examples in which disordered regions are located either far from the attachment site or completely absent. These findings argue, at least in these specific cases, that the attachment of ubiquitin may function in part to physically destabilize the substrate in order to prepare it for subsequent hydrolysis by the proteasome.

For proteins destined for degradation, covalently attached poly-ubiquitin chains function as physical tags that are recognized by receptors located on the proteasome.[20] Deubiquitinase enzymes (DUBs) associated with the proteasome recognize, cleave, and ultimately function to recycle ubiquitin for reuse in any of the cellular processes described above. Ongoing cycles of ubiquitination/deubiquitination are inherently dynamic and entail a large number of enzymes, many of which are still being discovered. Ubiquitin C-terminal hydrolase L3 (UCH-L3) is a cytosolic deubiquitinase that is not physically associated with the proteasome.[21−23] Although the precise biological function of UCH-L3 is not known, it is potentially involved in certain physiological processes[24−29] and has also been implicated in a number of cancer studies.[30−33] A consistent picture is emerging that at least one of the roles for UCH-L3 is the hydrolysis of small peptide extensions or chemical adducts from the C-terminus of ubiquitin that may remain following proteasomal processing.[21] Thus, a possible function of UCH-L3 is to cleanup, prepare, and recycle intact ubiquitin for subsequent rounds of ubiquitination.

Analysis of UCH-L3 substrate specificity demonstrated that it does not show activity toward linear Lys48- or Lys63-linked ubiquitin chains but instead hydrolyzes peptides or proteins linearly α-linked through the C-terminus of ubiquitin.[21] A substrate size preference was also demonstrated as UCH-L3 failed to hydrolyze larger proteins from ubiquitin such as β-galactosidase, cytochrome-C, and lysozyme.[21,22] A possible physical means by which size discrimination is achieved was revealed when the crystal structure of UCH-L3 was solved.[34,35] In addition to similarities with the papain family of cysteine proteases, including an active site catalytic triad, a striking feature of its structure is a unique ∼20 residue loop that spans the enzyme's active site. It is believed that this active site loop functions to restrict or filter the size of the substrate attached to the C-terminus of ubiquitin. The physiological relevance of this has not been determined, but one can readily envision that evolution would select for UCH-L3 to clear small peptides from ubiquitin yet not be able to cleave ubiquitin itself off physiologically important ubiquitin chains, such as linear tri- and diubiquitin. The diubiquitin version of ubiquitin is biologically relevant as it has been shown to interact with critical regulatory proteins (e.g., NEMO) of an important transcription factor complex (i.e., the NFκB complex). This protein complex functions to mediate gene expression in response to various physiological processes such as immune stimulation, inflammation, cell adhesion, and cell survival.[36] In one particular study, a yeast two-hybrid screen was used to isolate tandem diubiquitin (Ub-Ub) and triubiquitin molecules as interacting proteins with the NFκB regulator NEMO.[37] In a separate study, a cocrystal structure revealed that an interaction motif of NEMO forms a heterotetrameric complex with two linear di-ubiquitin molecules[38] Linear di-ubiquitin (Ub-Ub) was included in our studies to gain further insight into the substrate filtering selectivity of the UCH-L3 active site crossover loop.

Although it appears clear that the crossover loop restricts substrates based on size, it is not known what the actual size limitation is, and for that matter, if size is the only physical

dx.doi.org/10.1021/bi5006317 | *Biochemistry* 2014, 53, 8031−8042

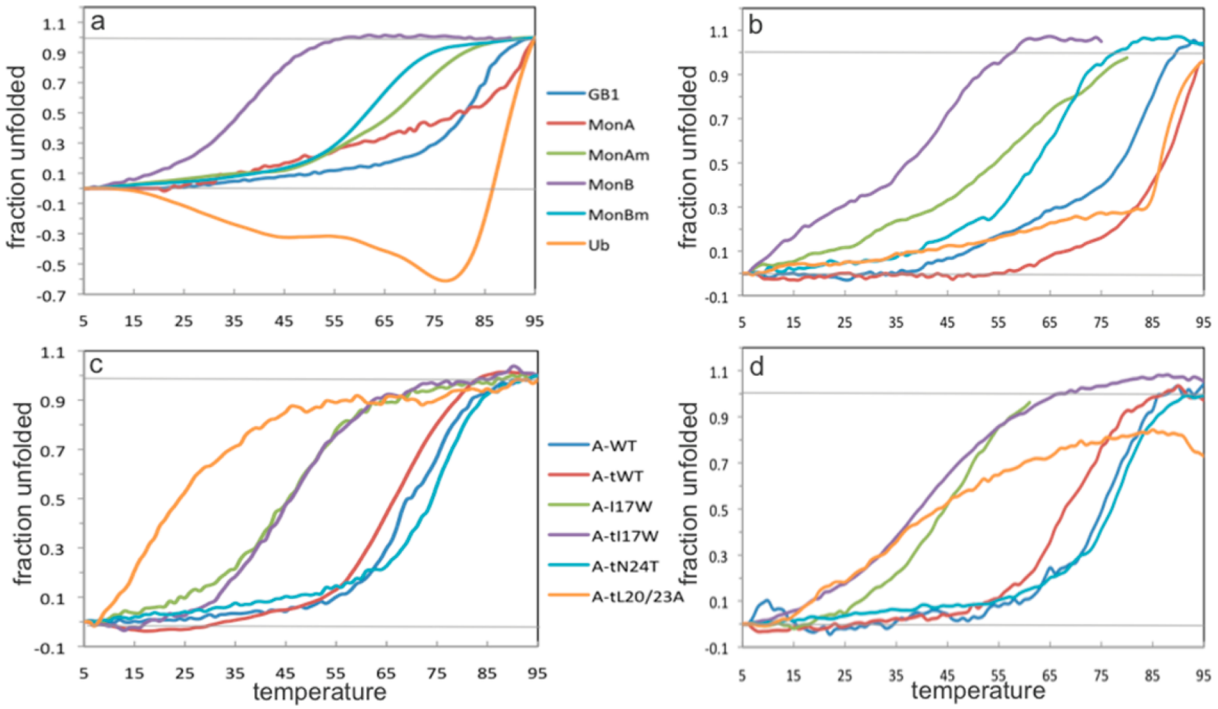

Figure 2. CD monitored thermal denaturation of free and ubiquitin-fused Gβ1 and SpA_B Variants. Panels (a and b) correspond to Gβ1 variants and panels (c and d) to SpA_B variants (A-WT is the nontruncated version of SpA_B-WT). Panels (a and c) are the thermal melts of the free domains, and panels (b and d) are those of the ubiquitin-fused domains. The colors in panels (a and b) correspond to the same Gβ1 variants, and the colors in panels (c and d) are the same for the SpA_B variants. MonAm corresponds to Monomer A (Y45A) and MonBm to Mononer B (A45F). The thermal melt for free ubiquitin is shown in orange in panel (a) and that for Ub-Ub is shown in orange in panel (b).

property restricted by the crossover loop. In addition, a minor paradox reported in the work by Larsen et al. is that UCH-L3 is able to cleave two naturally α-linked ribosomal proteins from the C-terminus of ubiquitin, which consist of 52 and 80 amino acids, yet it cannot cleave ubiquitin (76 amino acids) to any degree from α-linked di-ubiquitin. They also demonstrated that the addition of DNA to the ribosomal protein hydrolysis reaction reduced the hydrolysis of the Ub-CEP52 substrate (the 52 amino acid substrate) by UCH-L3. They speculated that, as with other nucleic acid binding proteins that become more ordered upon complex formation with nucleic acids,[39,40] the ubiquitin-linked ribosomal protein likely gains structural order upon binding DNA, and, in addition to associated size increase, greater order may contribute to the observed reduction in UCH-L3 hydrolysis. This was the first indication that a factor other than size may come into play regarding UCH-L3 substrate selectivity. Here we demonstrate, in the context of a series of engineered substrates, that substrate selectivity of UCH-L3 is not only based on size but also the thermal stability of α-linked test variants, and we speculate that this may be one reason why ubiquitin itself has such a high thermal stability ($T_m \approx 88$ °C).

MATERIALS AND METHODS

Protein Expression and Purification. The genes for the β1 domain of streptococcal protein G (Gβ1-WT), the B domain of staphylococcal protein A (SpA_B-WT), in addition to mutant variants and ubiquitin fusions, were generated using standard PCR methods and cloned in the expression vector pET19b (Novagen). *Escherichia coli* strain BL21 (DE3) was chemically transformed with the correspondent plasmids and grown on LB media to an optical density of 0.6−0.8 at 600 nm, and protein production was induced for 3 h by adding IPTG to a final concentration of 1 mM. Purification of Gβ1-WT and variants has been described.[41] N-Terminally polyhistidine-tagged ubiquitin-Gβ1 fusions were purified as follows: cell pellets obtained postinduction were resuspended in lysis buffer (50 mM NaH_2PO_4, 300 mM NaCl, 25 mM imidazole, pH 8.0) and lysed by sonication. The lysate was centrifuged at 10 000 rpm for 15 min to remove cell debris and then heated for 5−10 min at 85 °C to precipitate unwanted proteins. Precipitated material was removed via centrifugation for 15 min at 13 000 rpm at 4 °C. Cleared supernatant was applied to a metal affinity resin column, washed with resuspension buffer, and eluted with 250 mM imidazole. Fusions were concentrated and buffer exchanged into 25 mM sodium phosphate, 10 mM DTT, pH 6.8. Purification of ubiquitin-SpA_B fusions followed a similar approach: the cell pellet was resuspended in 1× PBS (137 mM NaCl, 2.7 mM KCl, 10 mM Na_2HPO_4, 1.8 mM KH_2PO_4, pH 7.4) and applied to affinity column as described above. Proteins were eluted with 50 mM NaH_2PO_4, 300 mM NaCl, 250 mM imidazole, pH 8.0. Fusions were concentrated and buffer exchanged into 25 mM sodium phosphate, 10 mM DTT, pH 6.8. N-Terminally polyhistidine-tagged UCH-L3 was purified in a similar fashion as ubiquitin fusions, but the heating step was omitted and lysis buffer consisted of 20 mM sodium phosphate, 500 mM sodium chloride, 20 mM imidazole, pH 7.4. UCH-L3 was eluted with resuspension buffer plus 500 mM imidazole and buffer exchanged into in 20 mM sodium phosphate, 0.5 M sodium chloride, and 10 mM DTT, pH 7.4. The free (nonfused) SpA_B-WT and SpA_BI17W variants were purchased from a commercial vendor (Peptide 2.0 Inc.) and purified by HPLC. The other SpA_B variants were expressed as ubiquitin fusions in *E. coli*. The attached ubiquitin was N-terminally

dx.doi.org/10.1021/bi5006317 | *Biochemistry* 2014, 53, 8031−8042

polyhistidine-tagged and fusion were purified using metal affinity as described above. To obtain the free SpA_B variants, the purified fusions were incubated with UCH-L3 for 12 h at 37 °C and passed through a metal affinity resin column to retain the polyhistidine-tagged ubiquitin and UCH-L3. Protein concentrations were measured by suspending each protein in 6 M guanidine hydrochloride, using standard A_{280} extinction coefficients for the tryptophan and tyrosine residues.

Circular Dichroism. CD data were collected on a Jasco-810 spectropolarimeter equipped with a thermoelectric unit using a 0.1 mm path-length cell. Protein concentrations were 50 μM and the buffer consisted of 50 mM sodium phosphate at pH 6.5. Far-UV spectra were acquired in continuous mode at 25 °C with 1 nm bandwidth and a 4 s response time. Thermal melts were monitored at 218 nm for the Ub-Gβ1-WT fusions, the Ub-SpA_B fusions, and for the Gβ1-WT variants and 208 nm for the SpA_B-WT and variants. For thermal denaturation curves the data were normalized by linearly shifting all points such that $[\theta]_{218}$ value at 5 °C equaled zero. A scaling factor was obtained for each set by dividing the maximum $[\theta]_{218}$ value for all sets at 95 °C by the $[\theta]_{218}$ value at 95 °C for each set. Data points for each set were scaled by the unique scaling factor calculated for each set and scaled to a value of one for the fully unfolded signal. For the CD thermal melt data presented in Figure 2, a simple exponential smoothing function was applied for the curves that correspond to the Ub-Gβ1-WT and Ub-SpA_B fusions.

UCH-L3 Hydrolysis of Ubiquitin Fusions. To assess the catalytic properties of UCH-L3 against the engineered ubiquitin fusions, we first performed cotranslational assays in which the expression of both the enzyme and the substrates takes place simultaneously in *E. coli*. This was accomplished by engineering a two-plasmid system with compatible origins of replication into which the genes for the enzyme and the substrates were cloned. After cotransformation of BL21 (DE3) *E. coli* with both plasmids, protein production was induced by addition of IPTG to a final concentration of 1 mM. Hydrolysis of the substrates was analyzed at different time points using SDS-PAGE. The extent of substrate hydrolysis by UCH-L3 for the in vitro assays was measured by incubating different concentrations of pure enzyme with 70 pmol of pure substrate in 25 mM phosphate buffer, 10 mM DTT, pH 6.8 with 0.5 μg of BSA added as an internal loading control. Reactions were incubated at 37 °C for 30 min. To determine the 50% hydrolysis time point ($t_{1/2}$), 4.2 pmol of enzyme was incubated with 70 pmol of substrate, and samples were collected at several time points. For both in vivo and in vitro assays, reactions were stopped by the addition of protein sample loading buffer and heated for 10 min at 95 °C. Samples were resolved by 15% SDS-PAGE, and relative intensity of the nonhydrolyzed substrate band was determined using ImageJ software. The $t_{1/2}$ values were calculated from a graph of log (band intensity) versus reaction time.

RESULTS

Nomenclature and Design of Gβ1 Variants, SpA_B Variants, and Ubiquitin Fusions. The hydrolysis rates of UCH-L3 were measured against 11 engineered protein substrates (α-linked through the C-terminus of ubiquitin) that are of similar molecular weight yet differ in thermal stabilities and secondary structure composition. The genes of the 11 designed protein substrates were cloned downstream of the gene for human ubiquitin and expressed as α-linked linear ubiquitin fusions. The test protein variants primarily fall into two groups: (1) variants of the β1 domain of streptococcal protein-G (56 amino acids and referred to as Gβ1-WT) and (2) variants of the B domain of staphylococcal protein-A (59 amino acids and referred to as SpA_B-WT). The Gβ1 variants consist of a β-sheet made up of four strands and an overlying α-helix (Supporting Information Figure 1a, blue), whereas the SpA_B variants consist of three-helix bundles (Supporting Information Figure 1b, green). A central α-helix is located in the same relative position in both Gβ1-WT and SpA_B-WT where amino acid identities occur at five of 15 positions; however there is no discernible sequence or structure homology between these two proteins.[42] The hydrolysis rates of UCH-L3 were tested against five ubiquitin fusions with Gβ1 variants, and six with SpA_B variants.

In addition to the 11 substrates described above, a variant in which ubiquitin is linearly expressed C-terminally to itself (i.e., Ub-Ub), and a variant that consists of Ub-Ub with a 22 amino acid extension, were also tested in the context of UCH-L3 hydrolysis. The Ub-Ub-22 variant was inadvertently created when a spontaneous mutation of the stop codon in the gene for the Ub-Ub linear dimer caused a read-through that terminated with a second stop codon further downstream within the expression vector. The 22 amino acid extension is made up of a random sequence of amino acids (i.e., RIRLLTKPERKL-SWLLPPLSNN) and is not expected to consist of stable structural elements. The Gβ1 and SpA_B variants were engineered to have variable melting temperatures while maintaining their overall three-dimensional structures. The rationale for, and the means by which these were engineered, are described in the Supporting Information.

Thermal Stabilities of the Engineered Substrates. The thermal stabilities of free ubiquitin, linear di-ubiquitin (Ub-Ub), all free Gβ1 and SpA_B test variants, and all test variants fused to the C-terminus of ubiquitin were measured using far ultraviolet (UV) circular dichroism (CD) spectroscopy.

Ubiquitin. The folding and unfolding properties of ubiquitin have previously been studied in detail, and our results confirm the relative thermostable nature of this molecule which has a measured T_m of ~88 °C.[43,44] In the case of the CD thermal melt data for both free ubiquitin (Figure 2a, orange curve) and the tandem Ub-Ub fusion (Figure 2b), there are significant and interesting differences when comparing the respective melting curves. The CD melting data for free ubiquitin confirms that it is a protein that undergoes cold denaturation[43] as a gradual increase in secondary structure signal (decrease in CD signal) is observed when the temperature is increased from 20 °C to ~76 °C. Slight precipitation was observed for the free ubiquitin sample after completion of temperature unfolding data collection.[44] Comparison of CD scans before and after obtaining the melting curve indicates that unfolding is likely reversible. In the case of the thermal melt data for the tandem Ub-Ub fusion, there are large differences in the preunfolding baseline in comparison to that of monomeric ubiquitin. Prior to denaturing (which occurs at approximately the same temperature as free ubiquitin), the CD signal for the Ub-Ub fusion gradually increases until just past 85 °C where the signal sharply increases in response to loss of secondary structure. The increase in the baseline signal prior to unfolding may be indicative of higher order structure especially as linear di-ubiquitin (Ub-Ub) molecules have be shown to form a heterotetrameric complex with a regulator of transcription in vivo.[36,38]

dx.doi.org/10.1021/bi5006317 | *Biochemistry* 2014, 53, 8031−8042

Free Gβ1 and SpA$_B$ Test Variants. CD spectra (collected from 190 to 280 nm) for the Gβ1 mutant variants indicate that the general α/β fold for the five variants is maintained and thus suggest that the introduced mutations do not significantly alter the overall Gβ1 fold. Thermal unfolding curves for the Gβ1 variants monitored at 218 nm confirmed previous findings in relationship to the importance of position 45 for the overall stability of Gβ1-WT (Figure 2a and Table 1).[41] CD spectra collected on free SpA$_B$-WT and five variants also indicate that the overall helical composition is maintained and that there are no obvious structural perturbations for the SpA$_B$ test variants. Except for the significantly destabilized double mutant (i.e., tSpA$_B$L20A/L23A), the CD spectra are highly similar (Supporting Information). Thermal melts were performed on all the SpA$_B$ variants (Figure 2c), and the resulting melting temperatures are listed in Table 2.

Table 1. T_m of Ubiquitin, Gβ1 Variants, and N-Terminal Ubiquitin Fusions[a]

free protein	T_m (°C)	Ub-fused protein	T_m (°C)
ubiquitin	88.5	Ub-Ub	85
protein Gβ1-WT[b]	85	Ub-Gβ1-WT	80.2
monomer A[b]	>100	Ub-MonA	90.7
monomer A(Y45A)	68.7	Ub-MonA(Y45A)	56.6
monomer B[b]	38	Ub-MonB	31.2
monomer B(A45F)	62.5	Ub-MonB(A45F)	59.8

[a]Average difference between free variant and variant fused to Ub = 7.2 °C ± 3.7. [b]Data from Barakat et al.[41]

Table 2. T_m of SpA$_B$ Variants and N-Terminal Ubiquitin Fusions[a]

free protein	T_m (°C)	Ub-fused protein	T_m (°C)
tSpA$_B$I17W	42	Ub-tSpA$_B$I17W	38
tSpA$_B$-WT	67	Ub-tSpA$_B$ −WT	67
SpA$_B$I17W	45	Ub-SpA$_B$I17W	43
SpA$_B$-WT	70	Ub-SpA$_B$-WT	72
tSpA$_B$L20A/L23A	<20	Ub-tSpA$_B$L20A/L23A	<20
tSpA$_B$N24T	75	Ub-tSpA$_B$N24T	76

[a]Average difference between free variant and variant fused to Ub = 1.8 °C ± 1.5.

Thermal Denaturation of Ubiquitin Fusions. In addition to determining the melting temperatures of all single "free" SpA$_B$ and Gβ1 test variants, the melting temperatures of all fused proteins, in which each variant was expressed as a C-terminal fusion to ubiquitin, were also measured. Interestingly, in almost all cases the measured melting temperatures of the fusion proteins are very close to the melting temperature of the attached SpA$_B$ and Gβ1 variants and not to that of ubiquitin (Tables 1 and 2). A potential model for this finding is provided in the Discussion. In almost all cases, the CD thermal denaturation data collected on the Gβ1 and SpA$_B$ ubiquitin fusions was generally not as smooth as the data collected on the free variants. In addition, for two Gβ1variants (i.e., Ub-MonB, Ub-MonA (Y45A)) and one SpA$_B$ variant (i.e., Ub-SpA$_B$ I17W), the CD signal degraded after approximately 65−75 °C, and precipitate was observed for these variants after completion of the thermal melts. Although this was the case, it did not preclude our ability to estimate the approximate melting temperatures for these variants. It is assumed that the dynamic structure of ubiquitin combined with the low to moderate melting temperatures of these variants may be the origin of the greater fluctuations in the signal and the observed aggregation. This is not surprising especially in light of the fact that two of the Gβ1 variants (i.e., monomer A and monomer B) were engineered to form a heterodimeric structure[45] and that less stable variants of Gβ1 have been demonstrated to form amyloid fibers.[46] The inherent tendency to self-associate, combined with being tethered to the dynamic and fluid structure of ubiquitin, may be the reason for the increased data fluctuation as well as the degradation of the CD signal for three variants in the mid to high temperature range.

In the case of the SpA$_B$ variants, the melting temperatures of the ubiquitin-SpA$_B$ fusions very closely match those of the free test proteins (Table 2). The average difference between the free test proteins and the associated ubiquitin-SpA$_B$ fusions is 1.8 °C (±1.5 °C). For the Gβ1 variants, the melting temperatures of the fusions were typically somewhat lower than that of the single test proteins (Table 1). In this case, the average difference between the free test proteins and the associated ubiquitin fusions is 7.2 °C (±3.7 °C). In all cases, the thermal unfolding curves for all fusions appear biphasic and thus indicate no significant unfolding intermediates. These findings are in agreement with the two-state unfolding model observed when the individual components of the fusions (i.e., ubiquitin and Gβ1) were subjected to thermal denaturation analysis.[44,47] This suggests that the ubiquitin fusion proteins unfold cooperatively, as opposed to the domain of lower stability unfolding first followed by the unfolding of the more stable domain. This is the case even when the C-terminal test protein is significantly destabilized.

UCH-L3 Hydrolysis. *Hydrolysis of Ubiquitin Fusions Assessed by Co-Translational Assays.* A cotranslational assay where UCH-L3 and the ubiquitin fusion substrate are coexpressed in *E. coli* was initially used to screen UCH-L3 hydrolysis activity in vivo. Thirty minutes after induction increasing amounts of intact Ub-Gβ1-WT (T_m ≈ 80 °C), Ub-MonA (T_m ≈ 91 °C) and Ub-MonA(Y45A) (T_m ≈ 57 °C) accumulated, and no products of hydrolysis were observed for these variants even after 180 min (Figure 2, Supporting Information). In the case of the Ub-MonB variant (T_m ≈ 31 °C), only limited amounts of this fusion are visible 60 min after induction, while extensive products of hydrolysis are shown to accumulate. On the other hand, a more stable variant of this substrate, Ub-MonB(A45F) (T_m 60 °C), is only partially hydrolyzed and accumulates in a pattern similar to that of Ub-Gβ1-WT, Ub-MonA, and Ub-Mon(Y45A). According to Larsen et al., UCH-L3 hydrolyzes peptides attached to the C-terminus of ubiquitin more efficiently if the enzyme is present during the synthesis of the substrate, before the C-terminal extension has a chance to fold into a stable domain.[48] This is a reasonable assumption; however, we did not observe this except possibly in the case of the Ub-MonB variant (T_m ≈ 31 °C) and to lesser extent for the Ub-MonB(A45F) variant (T_m ~60 °C) as the other three fusions were not observed to be hydrolyzed in the context of this in vivo screen. Although the convenience of this format in analyzing hydrolysis is clear, a major drawback is that expression levels for the enzyme and substrates cannot be precisely controlled. The results described above could be due to unequal enzyme or substrate expression within the bacterial cultures. As we desired to more accurately characterize UCH-L3 hydrolysis rates, the potential unequal expression of enzyme and substrates is relevant. This is

dx.doi.org/10.1021/bi5006317 | *Biochemistry* 2014, 53, 8031−8042

especially true when the differences in thermal stabilities between protein substrates are small, as in the cases of Ub-MonA(Y45A) and Ub-MonB(A45F) which differ by only ~7 °C (Table 1).

In Vitro Analysis of the UCH-L3 Hydrolysis. To more accurately assess differences in UCH-L3 hydrolysis rates as a function of substrate thermal stability, the enzyme and all ubiquitin fusion variants were expressed separately, purified to homogeneity, and tested in vitro. Individual fused proteins from the two sets of purified substrates were separately incubated with UCH-L3, and the hydrolysis rates were estimated based on SDS-PAGE analysis. Overall the observed hydrolysis rates strongly correlate to the thermal stability of the C-terminally attached Gβ1 and SpA_B test variants (Figures 3 and 4). In lieu

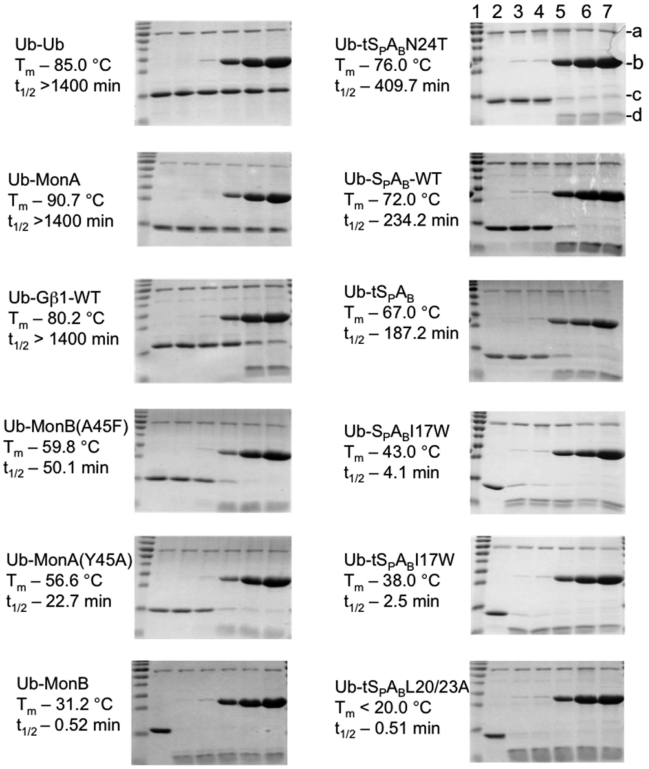

Figure 3. In vitro UCH-L3 hydrolysis of ubiquitin N-terminal fusions. Increasing amounts of UCH-L3 and fixed amounts of substrates were reacted for 30′ at 37 °C. The melting temperatures (T_m) and the $t_{1/2}$ values for all fusions are listed below each variant name. Five of the six panels on the left correspond to Ub-Gβ1 substrates (top left - Ub-Ub) and those on the right to Ub-S_PA_B substrates. Description of the various gel bands are included in the upper right-hand panel: (a) BSA loading standard; (b) increasing amounts of UCH-L3 (lane 2—0 pM, lane 3—3.5 pM, lane 4—7.0 pM, lane 5—70.0 pM, lane 6—140.0 pM, lane 7—278.0 pM); (c) nonhydrolyzed, ubiquitin-fused substrates; (d) hydrolysis products (ubiquitin and free test variants). Lane 1 contains molecular weight standards (10, 15, 25, 35, 45, 55, 70, 100, and 130 kDa).

of a real-time assay that would enable the measurement of specific catalytic parameters, the extent of hydrolysis was assessed using densitometric analysis of SDS-PAGE gels of remaining unreacted substrate compared to a control in which no enzyme was added. This allowed us to estimate the percentage of substrate that was not hydrolyzed by UCH-L3 (Supporting Information Figure 5). This assay revealed that, for both sets of substrates, the extent of hydrolysis differed between

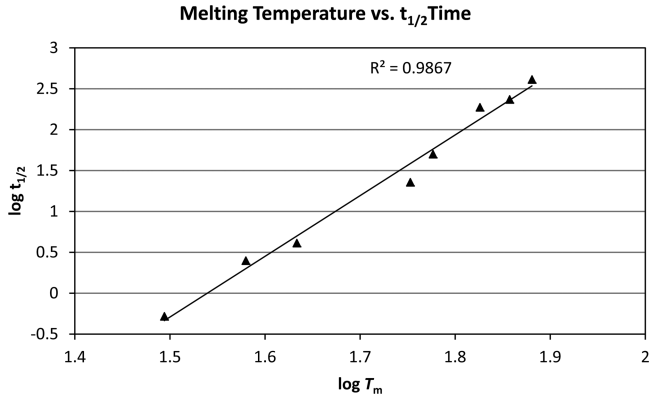

Figure 4. Plot of the logarithm of the melting temperature versus the logarithm of the time to reach approximately 50% hydrolysis by UCH-L3 for all variants that were hydrolyzed in less than 24 h (<1440 min).

variants and was strongly correlated to the thermal stabilities of the C-terminally attached test variant.

UCH-L3 Hydrolysis of Ub-Gβ1 Variants. The reaction of 10.0 pmol of UCH-L3 with 70.0 pmol of Ub-Gβ1-WT ($T_m \approx$ 80 °C) or Ub-MonA ($T_m \approx$ 91 °C) resulted in no observable hydrolysis even when the incubation periods were extended past 24 h (data not shown). In contrast, hydrolysis of Ub-MonA(Y45A) ($T_m \approx$ 57 °C) and Ub-MonB(A45F) ($T_m \approx$ 60 °C) occurs within minutes and Ub-MonB ($T_m \approx$ 31 °C) is hydrolyzed within seconds. In addition to visual inspection of the gels, a semiquantitative comparison was performed based on densitometric analysis of unreacted substrates which enabled the estimation of the time point associated with 50% hydrolysis of substrates ($t_{1/2}$ value). This analysis demonstrated that the hyperthermostable variants such as Ub-Gβ1-WT and Ub-MonA require greater than 1440 min (24 h) to reach $t_{1/2}$ under these conditions, whereas the mesothermostable variants such as Ub-MonA(Y45A) and Ub-MonB(A45F) have $t_{1/2}$ values of 50.1 and 22.7 min, respectively. The variant of lowest thermal stability Ub-MonB is hydrolyzed rapidly with a $t_{1/2}$ value of 0.52 min.

Because of this wide disparity in hydrolysis rates, it was difficult to determine conditions in which the rates could be effectively compared for the different ubiquitin-linked substrates. In an attempt to address this issue, a second series of assays were performed in which a fixed amount of substrate (i.e., 70 pmol) was incubated with increasing amounts of the UCH-L3 enzyme (Figure 3). The reactions were incubated at 37 °C and quenched after 30 min. For the subset of substrates derived from Ub-Gβ1, 3.5 pmol of enzyme was enough to hydrolyze the least stable Ub-MonB variant, while variants of medium stability (i.e., Ub-MonB(A45F)) exhibited only a slight degree of hydrolysis, and for the more stable variants, Ub-Gβ1-WT and Ub-MonA, no hydrolysis was observed.

As illustrated in Figure 3, when the amount of enzyme is increased the amount of observable hydrolysis also increases for the variants of low to mid thermal stability. For example, at 7.0 pmol of enzyme the Ub-MonB variant was fully hydrolyzed, whereas only ~24% of the Ub-MonB(A45F) was hydrolyzed. At this enzyme concentration, only ~5% of the more stable Ub-MonA(Y45A) variant was hydrolyzed, whereas the variants of highest stability, Ub-Gβ1-WT, Ub-MonA, and Ub-Ub remained essentially unreacted. Using 70.0 pmol of enzyme, the variants of medium thermal stability, Ub-MonA(Y45A) and Ub-MonB(A45F), were significantly hydrolyzed, while the stable

dx.doi.org/10.1021/bi5006317 | *Biochemistry* 2014, 53, 8031−8042

Ub-Gβ1-WT variant began to show evidence of hydrolysis with ~68% remaining. For the hyperthemostable variant Ub-MonA, again no appreciable hydrolysis was observed. At 140.0 pmol of enzyme, Ub-MonB(A45F) was essentially fully hydrolyzed, Ub-MonA(Y45A) was almost fully hydrolyzed with about 14% remaining, and the Ub-Gβ1-WT variant was appreciably hydrolyzed with ~34% remaining. At 140.0 pmol of enzyme Ub-MonA finally showed evidence of hydrolysis with 88% remaining after 30 min. At the highest amount of UCH-L3 assayed (i.e., 278.0 pmol), 28% of Ub-Gβ1-WT remained after 30 min and Ub-MonA was reduced to ~84%. As seen in Figure 3 (top left panel), there is no observable hydrolysis of the linear Ub-Ub variant at any of the enzyme concentrations tested.

UCH-L3 Hydrolysis of Ub-SpA$_B$ Variants. A parallel analysis was performed for the engineered variants derived from the Ub-SpA$_B$ fusions (Figure 3, right panels) and revealed an outcome that is similar to the results obtained for the Ub-Gβ1 variants. At the lowest concentration of enzyme tested, 3.5 pmol, the relatively unstable variants, Ub-tSpA$_B$L20A/L23A (T_m < 20 °C), Ub-tSpA$_B$I17W (T_m ≈ 42 °C), and Ub-SpA$_B$I17W (T_m ≈ 45 °C), exhibited extensive hydrolysis (~94.7, ~93.1%, ~88% respectively), whereas the more stable variants Ub-SpA$_B$-WT (T_m 70 °C), Ub-tSpA$_B$ (T_m 67 °C), and Ub-tSpA$_B$N24T (T_m 75 °C) showed no evidence of hydrolysis. Minor but consistent differences were observed for the truncated versus nontruncated SpA$_B$ variants. At 7.0 pmol of enzyme the nontruncated Ub-SpA$_B$-WT variant showed no evidence of hydrolysis, while its truncated version, Ub-tSpA$_B$, showed slight evidence of hydrolysis. The additional amino acids at the termini of the nontruncated SpA$_B$ variants appear to confer a slight increase in thermal stability and a corresponding slight decrease in UCH-L3 hydrolysis. At 7.0 pmol of enzyme the remainder of the unstable variants appear to be fully hydrolyzed, while the most stable variant, tSpA$_B$N24T, again showed no evidence of hydrolysis. Unlike the more stable Ub-Gβ1 variants, there is evidence for fairly significant hydrolysis when 70.0 pmol of enzyme was incubated with all of the SpA$_B$ variants. This is apparently due to the differences in the melting temperatures, but differences in secondary structure content may also play a role when comparing the fully α-helical SpA$_B$ variants to the Gβ1 variants (which contains a four stranded β-sheet). At 70.0 pmol of enzyme most of the Ub-SpA$_B$ variants except for the three most stable (with T_m's of 67 °C, 70 °C, and 75 °C) are fully hydrolyzed. Under these conditions the most stable variants, Ub-SpA$_B$-WT, Ub-tSpA$_B$, and tSpA$_B$N24T, were significantly hydrolyzed with approximately 12.5%, 17%, and 22% remaining, respectively. Finally all of the Ub-SpA$_B$ variants are essentially fully hydrolyzed when 140.0 and 278.0 pmol of the UCH-L3 enzyme was incubated with the substrates.

UCH-L3 Hydrolysis of the Linear Ub-Ub Fusion and Ub-Ub-22. The rate of hydrolysis of ubiquitin fusions by UCH-L3 is relatively slow when the attached Gβ1 and SpA$_B$ substrates possess relatively high thermal stabilities. Considering this we theorized that the lack of hydrolysis for the Ub-Ub fusion by UCH-L3 could possibly be due to the high thermal stability of ubiquitin.[49,50] The Ub-Ub fusion is especially interesting because this protein occurs naturally,[50] and the two ubiquitin units are fused in the same manner as all the other fusions studied thus far (C- to N-terminus). The Ub-Ub fusion is a relatively stable variant (T_m ≈ 85 °C), and thus it was tested to determine if it could be hydrolyzed by UCH-L3 under the same experimental conditions used to characterize the other fusions. In the assay in which a fixed amount of enzyme and substrate were incubated for various time periods, the Ub-Ub fusion was not hydrolyzed even after an incubation period of 24 h. Similarly in the experiment where enzyme-concentration is varied, the Ub-Ub fusion is not hydrolyzed when incubated with up to 278.0 pmol of UCH-L3 (Figure 3, top left panel). Under these conditions the two most stable ubiquitin fusions derived from Gβ1, Ub-MonA and Ub-Gβ1-WT showed evidence of hydrolysis and therefore the Ub-Ub variant proved to be the most hydrolytically stable substrate.

In addition to the Ub-Ub fusion an additional variant with a 22 amino acid C-terminal extension (Ub-Ub-22) was tested in UCH-L3 hydrolysis assays. Short, unstructured extensions attached to the C-terminus of ubiquitin have proved to be good substrates for UCH-L3,[48] and thus it is of interest to determine if this property remained when such a leaving group was preceded by not one but two ubiquitin moieties. In the context of the time-dependent assay and the concentration-dependent assay, it was found that the 22 amino acid extension was readily cleaved from Ub-Ub-22 with a $t_{1/2}$ value of 1.3 min (Figure 3, Supporting Information). The $t_{1/2}$ value of Ub-Ub-22 is comparable to that of Ub-MonB (0.52 min), the least thermally stable Gβ1 construct. Although we did not determine the thermal stability of Ub-Ub-22, two possible arguments that may explain such similar $t_{1/2}$ values are the small size and unstructured sequence of the 22-mer random amino acid sequence that derives from the multiple cloning site of the vector used to clone Ub-Ub. Therefore, we would not expect that the 22-mer would have extensive secondary structure or that it is folded to any appreciable extent. The high activity of UCH-L3 in cleaving the 22-mer off the distal ubiquitin in the context of the ubiquitin linear dimer suggests that this enzyme may possibly have evolved to cleave C-terminal peptides from both mono-ubiquitin and poly-ubiquitin chains.

DISCUSSION

The ongoing characterization of the substrate specificity and catalytic properties of the deubiquitinating enzyme UCH-L3 is significant for a number of reasons. The ever expanding roles that elements of the ubiquitin/proteasome system play in cytosolic protein stasis illustrate the overall importance of the enzymes involved in this essential regulatory process. A potential role for the human enzyme UCH-L3 is the cleavage of small protein/peptide extensions off the C-terminus of ubiquitin that may remain following proteasomal processing.[21] In addition to in vivo roles, UCH-L3, in combination with ubiquitin (or the closely related SUMO-fusion expression system), functions as a highly effective biotechnological tool that enables the production of proteins and peptides that are difficult to produce in bacterial expression systems.[51−57] To potentially enhance its ability to function in this role, possibly through the use of protein design methods, we believe it is important to further characterize its substrate specificity and catalytic properties against a series of engineered substrates that are similar in size yet differ in another physical parameter such as thermal stability. To complement the evaluation of UCH-L3 substrate specificity, we examined the effects of fusion to ubiquitin on the biophysical properties of the engineered test proteins.

Thermal Denaturation of Ubiquitin Fusions. The melting temperatures were measured for all single "free" Gβ1 and SpA$_B$ test variants as well as the chimeric versions in which each test variant was expressed as α-linked C-terminal fusions to ubiquitin. Prior to the measurement of the melting

dx.doi.org/10.1021/bi5006317 | *Biochemistry* 2014, 53, 8031−8042

temperatures, it was not known what effect the fusing of small proteins to ubiquitin would have on the overall thermal stability of the resulting chimeras. For example, would the thermal stability of the fusion proteins average that of the nonfused test variant and ubiquitin or would the melting curve exhibit multiple phases that correspond to independent unfolding of each protein? An interesting result was observed upon determining the melting temperatures of the chimeric fusions. In almost all cases, the melting temperatures of the fusion proteins are very similar to the melting temperature of the attached SpA_B and Gβ1 variants and not to that of ubiquitin, suggesting little to no transference of stability from ubiquitin to the attached test variants (Tables 1 and 2). These results imply that, below their melting temperatures, there is likely no substantial physical interaction between ubiquitin and the attached engineered proteins. In a separate study, in which ubiquitin was fused to various ubiquitin interacting motifs (UIM), it was found that the fusions had melting temperatures that were increased by at least 10 °C relative to ubiquitin alone.[58] This finding is not surprising as the attached peptides (~25 residues) are helical UIM segments that have been demonstrated to physically interact with ubiquitin. The physical interactions between ubiquitin and the attached helix is likely the reason for the observed increase in the thermal stability of engineered ubiquitin/UIM fusions. In addition to the work on ubiquitin/UIM fusions, previous in silico approaches revealed that ubiquitin may function to induce protein instability when bound to natural in vivo targets and thus possibly assist the degradation process by the ubiquitin-proteasome system.[13] It was also observed that when proteins are tagged with ubiquitin for degradation by the UPS there is a bias for ubiquitination to occur in disordered regions, which indicates that the covalent attachment of ubiquitin likely does not function to increase the stability of targeted proteins.[19]

For our results, the average difference between the melting temperatures of the free SpA_B test proteins and the associated ubiquitin-SpA_B fusions is 1.8 °C (±1.5 °C), and for the Gβ1 variants the corresponding average difference is 7.2 °C (±3.7 °C). Although the biological relevance for this finding is not obvious, it may shed light on some of the unique biophysical properties of ubiquitin, properties that enable it to function in the myriad biological roles thus far described for this important protein. The melting temperature of free ubiquitin is relatively high (i.e., ~88 °C), and thus it is considered a hyperthermostable protein although it is found in many mesophilic organisms. In addition, it has been demonstrated in our laboratory, as well as in previous reports,[43] that ubiquitin is a protein that undergoes cold denaturation, i.e., during the thermal melt of free ubiquitin the CD signal is unique relative to most proteins in that it actually decreases when the temperature is raised from below 20 °C to ~76 °C, indicative of an increase in secondary structure content (Figure 2a, orange). The fact that there is an initial increase in secondary structure content as the temperature increases indicates that at lower temperatures there are atoms at residue positions that do not have fully formed secondary structure yet gain order with increasing temperature. This also implies that, for the atoms in those regions, there may be a subtle balance between enthalpic and entropic factors that ultimately give rise to the dynamic and fluid nature of ubiquitin.

Considerable research efforts have been reported on many aspects of ubiquitin function such as the ubiquitin code,[3] surface regions of other proteins that interact with ubiquitin (ubiquitin binding domains − UBD),[59−61] as well as its biophysical properties.[62] Although there is an extensive body of literature covering these important topics, there has been little discussion of potential roles for the regions of ubiquitin that contain relatively atypical secondary structure elements such as the small 3_{10} helix and a small stretch of β-strand found in proximity between residues 45 to 64 (Figure 5, black arrows). A

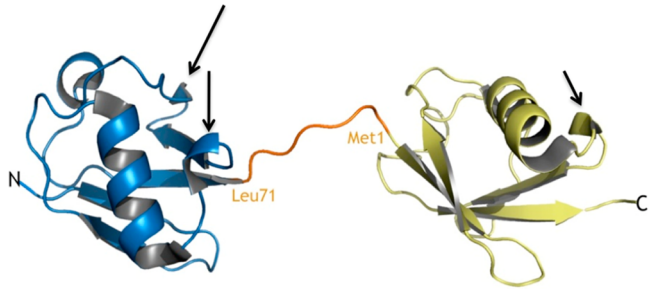

Figure 5. Structure of the linearly α-linked Ub-Ub dimer. The proximal ubiquitin is shown in blue and the distal ubiquitin is in yellow. In orange is the intervening stretch of residues that connects both ubiquitin units and extends ~7 amino acids, from Leu71 in the proximal moiety to Met1 in the distal. The linkage is partly disordered with high temperature factors, consistent with intrinsic flexibility.[18] The small 3_{10} helix and small stretch of β-strand are indicated with black arrows.

3_{10} helix has been described as a "parahelix" as it appears primed to be converted into a more common α-helix,[63] and thus it is considered an intermediate between a nascent and fully formed helix. There are no obvious roles for these elements, and thus they may exist solely as a consequence of the need for the structure of ubiquitin to maintain its overall fold plus a fairly extensive yet fluid hydrophobic core. These unusual structural features of ubiquitin may be related to our finding that the melting temperatures of our ubiquitin-test proteins usually match those of the less stable test variant and not ubiquitin.

The primary sequence of ubiquitin is extremely conserved as evidenced by the fact that there is 100% amino acid identity between humans and fruit flies (and many other organisms). Why did the process of evolution ultimately select a sequence for ubiquitin that confers relatively high thermal stability ($T_m \approx$ 88 °C) yet maintains a somewhat mobile, fluid-like nature? A well-established fact is that ubiquitin interacts with many different protein binding partners. Covalent and noncovalent interactions occur with members of the E1, E2, and E3 enzymes that are ultimately responsible for catalyzing the iso-peptide bond formed between ubiquitin and proteins targeted for degradation. The degradation process is completed after ubiquitin-bound proteins are recognized by receptors on the surface of the proteosome where deubuitinases recognize, cleave, and recycle ubiquitin. This raises the interesting biophysical question as to how this relatively small protein (76 amino acids) is able to form so many specific covalent and noncovalent interactions with different protein interaction partners. Insight as to how this is achieved is derived from a series of highly developed NMR experiments that definitively demonstrate that ubiquitin exists in solution as a conformational ensemble of moderately different structures.[64,65] Ubiquitin is able to fulfill its multiple roles by physically interacting with different binding partners in a process referred to as "conformational selection". As a particular conformer of

dx.doi.org/10.1021/bi5006317 | Biochemistry 2014, 53, 8031−8042

ubiquitin is recognized and bound by a binding partner the equilibrium distribution of different ubiquitin structures is altered in response to binding. The remaining free ubiquitin molecules repopulate the particular structure that binds the target protein thus giving rise to additional binding events.

How is ubiquitin able to exist as a conformational ensemble of different structures? This behavior necessitates an inherent plasticity for ubiquitin and thus there is likely a fine balance between the energies associated with the hydrophobic interactions within ubiquitin's core and the surrounding secondary structure elements. These properties provide a possible model as to why the ubiquitin fusions take on the melting temperature of the less stable attached test protein. As the temperature increases the attached variant begins to unfold and expose previously buried hydrophobic residues. This process is entropically unfavorable, as water molecules become ordered in proximity to exposed hydrophobic residues, and therefore it is possible that these newly exposed residues may be driven to interact or pack within hydrophobic regions of ubiquitin. This model may be unique to ubiquitin as its inherent conformational heterogeneity and fluidity may provide multiple areas of exposed hydrophobic surface patches. As there is likely a delicate balance between the energies associated with ubiquitin's hydrophobic core and the surrounding secondary structure elements (as evidenced by the atypical secondary structure elements described above), any interaction between exposed hydrophobic residues and hydrophobic regions on the surface of ubiquitin might destabilize its structure and induce the fusions to unfold at the observed lower temperatures. It is also tempting to speculate that the atypical secondary structure elements described above may be primed to form transient interactions with attached targeted proteins and thus may assist in the overall unfolding process.

Although the ubiquitin fusions described within are purely engineered constructs, and thus were not subjected to evolutionary selection over vast expanses of time, further insights into potential "cross-talk" between the fused domains may be inferred from studies performed on natural multidomain proteins. In one such study a combination minimalist (i.e., course-grained) and atomistic molecular dynamics approach was implemented to explore biophysical characteristics of multidomain folding of tethered immunoglobulin-like β-sandwich domains from fibronectin (i.e., FNfn9-FNfn10) and human titin (i.e., I27−I27).[66] Of particular relevance to our work are the studies in which the rigidity of the intervening linker was altered and analyzed to determine effects on domain stability. The results indicate a strong correlation between linker rigidity and domain stability, i.e., a more rigid linker correlates to lower overall stability of the attached domains. They suggest that a rigid linker functions to more closely couple the folding properties of the attached domains. For the engineered ubiquitin fusions studied in our laboratory, as for example the natural Ub-Ub variant, there is a ∼6−7 amino acid sequence separating ubiquitin and the attached test variants. The crystal structure of di-ubiquitin reveals that this sequence is extended and likely not very rigid and thus additional factors must come into play when considering the folding/unfolding properties of the ubiquitin fusions. In fact their findings demonstrated that the significance of stabilizing and destabilizing factors depends on case-dependent properties such as the size of the interface, the stability of each domain, as well as the length and rigidity of the linker. It is our belief that, in functioning as a molecular tag for many different cellular proteins, the particular sequence/structure of ubiquitin may impart unique properties on the resulting transient interface, and these properties likely differ from those of the more permanent interfaces found in multidomain proteins.

In a separate study, designed to emulate the "crowded" molecular conditions within cells, a protein (i.e., staphylococcal nuclease) was covalently cross-linked to itself with a series of chemical linkers that resulted in linker lengths that ranged from 10.5 to 21.3 Å.[67] Engineered dimers with relatively short linkers exhibited three-state denaturation behavior yet reverted back to two-state behavior with increasing linker length, thus implying a higher level of physical "cross-talk" between domains with short linkers. The authors note that, in contradiction to theoretical predictions (and in agreement with our findings), none of the engineered dimers were stabilized relative to monomeric versions of the mutant proteins. The amino-acid segment separating ubiquitin and our attached test variants consists of ∼6−7 residues. Using the standard peptide contour length of ∼3.8 Å per residue, the length associated with this "linker" (when fully extended) would be greater than 20 Å and thus likely limit "cross-talk" between domains during unfolding. For the engineered ubiquitin fusions this is clearly not the case as, even with its medium to long length linker, the melting temperatures of almost all test variants were altered upon fusion to ubiquitin. Thus, it is of high interest to experimentally ascertain if the versatile ubiquitin protein imparts unique properties on the interface created upon attachment to targeted proteins. The highly conserved ubiquitin sequence may have evolved to assist in the unfolding of the attached protein through enhanced cross-talk, which may be unique to ubiquitin and possibly correlated to its inherent fluidity and the aforementioned odd secondary structure elements. These elements are possibly primed to supply alterative backbone hydrogen-bond donor and acceptor groups and, in doing so, "soften" up the structure of the attached protein prior to the unfolding/threading that necessarily occurs at the proteasome.

UCH-L3 Hydrolysis Rates. A major finding of our work is that UCH-L3 hydrolysis rates for the different engineered substrates are very closely correlated to the thermal stabilities of each attached test protein substrate (Figures 3 and 4). This finding is in agreement with previous research conducted on the UCH-L3 hydrolysis for linearly (as well as nonlinearly) attached substrates derived from natural and engineered sources.[48] In this previous study UCH-L3 hydrolysis rates were measured against single amino acid substrates fused to the C-terminus of ubiquitin as well as peptide sequences derived from natural fusions between ubiquitin and two ribosomal proteins. Unlike most ribosomal proteins, which are expressed as individual gene products, two small ribosomal proteins, s27a and L40, are expressed as linear α-linked ubiquitin fusions.[68] The L40 and s27a gene products, excluding the 76 amino acid sequence for ubiquitin, consist of 52 (6.2 kDa) and 80 (9.4 kDa) amino acids, respectively. Both proteins contain an excess of basic residues, have calculated isoelectric points in excess of 10, and contain large stretches of hydrophilic regions made up primarily of charged residues. It is thought that these proteins, outside of the context of the stable ribosome structure, contain intrinsically disordered regions. The genetic fusing of ubiquitin to these small ribosomal proteins may function to confer greater in vivo stability via a mechanism similar to that in which recombinant ubiquitin fusion allows the generation of proteins that are difficult to express in *E. coli*. Ubiquitin's inherent stability may enable these small proteins to survive in the

dx.doi.org/10.1021/bi5006317 | *Biochemistry* 2014, 53, 8031−8042

cytosol until they are processed and achieve a stable conformation upon assembly within the intact ribosome.

The work reported by Larsen et al. demonstrated that the smaller ribosomal fusion (i.e., L40, referred to as Ub-CEP52) is readily cleaved from the C-terminus of ubiquitin yet the addition of DNA to the reaction restricted hydrolysis.[21] They rationalized that, since it is a nucleic acid binding protein Ub-CEP52 likely formed a complex with DNA and that binding resulted in increased stability, which subsequently blocked processing by UCH-L3. They also speculated that a factor other than size may also play an important role in UCH-L3 substrate selectivity. Our results demonstrate that the other key factor is the thermal stability of the substrates which may be one of the reasons evolution selected for a unique sequence for ubiquitin that confers relatively high thermal stability. However, thermal stability cannot be the only factor as linear diubiquitin (Ub-Ub) showed no evidence of hydrolysis even though its melting temperature (i.e., ∼85 °C) is ∼5 °C lower than the Ub-MonA variant and only ∼5 °C higher than the Ub-Gβ1-WT variant (both of which hydrolyze in the presence of an excess of UCH-L3 over longer periods of time). Larsen et al. demonstrated that UCH-L3 can process the smaller Ub-CEP52, but not the larger Ub-CEP80 in vitro yet hydrolysis was readily observed for Ub-CEP80 in cotranslational in vivo assays.[21] They rationalized that the Ub-CEP80 variant may have been cleaved as it was being synthesized and before it was fully folded. An alternative, and not necessarily exclusive interpretation, is that the size of the Ub-CEP80 variant may be near the limit imposed by the active site crossover loop and conditions within the in vivo assays were conducive to hydrolysis by UCH-L3. Thus, the relative size of ubiquitin (76 amino acids) may be close to the size limitation imposed by the crossover loop and therefore its high thermal stability may be essential to prevent uncontrolled cleavage of ubiquitin from in vivo targets or important ubiquitin signaling variants, such as linear Ub-Ub. Uncontrolled cleavage of ubiquitin by UCH-L3 from linear substrates would potentially derail functions associated with these forms of ubiquitination. During the process of evolution an amino acid sequence for UCH-L3 would have been selected for that would (1) recognize and bind ubiquitin and (2) facilitate the cleavage of small peptides and/or adducts from its C-terminus while not cleaving larger or more stable substrates such as di-ubiquitin. The unique sequence of ubiquitin may have evolved, in part, to have both the required size as well as high thermal stability in order to inhibit cleavage of linear di- or poly-ubiquitin substrates by UCH-L3 (and other deubiquitinases).

A strength of using the ubiquitin/UCH-L3 system for producing proteins/peptides in *E. coli* expression systems is that no "scar" amino acids remain at the N-terminus of the product after cleavage with UCH-L3 (i.e., UCH-L3 cleaves cleanly after the C-terminal glycine of ubiquitin). This is the primary reason we did not include a linker between the C-terminus of ubiquitin and the N-terminus of the Gβ1 and SpA_B test variants. We assume that an unstructured, extended linker would potentially lessen the temperature dependence of UCH-L3 cleavage. It is interesting to note that for the X-ray crystal structure of α-linked, linear di-ubiquitin there exists an extended and relatively unstructured stretch of amino acids between the two ubiquitin moieties (Figure 5). Although unstructured, this ∼6−7 amino acid segment still does not enable UCH-L3 to hydrolyze the linear di-ubiquitin which provides further evidence that the specific spatial requirements for proper orientation of substrates in its active site, mediated in part by the crossover loop, is precise yet disrupted by certain factors. Previous reports demonstrated that substrate size is a key factor, whereas our results strongly indicate that thermal stability also plays an important role in the substrate selectivity of UCH-L3.

■ ASSOCIATED CONTENT

Supporting Information

Detailed descriptions of the design of all engineered substrates, the design and testing of an extended UCH-L3 crossover loop, additional SDS-PAGE hydrolysis figures, and extended experimental section. This material is available free of charge via the Internet at http://pubs.acs.org.

■ AUTHOR INFORMATION

Corresponding Author

*E-mail: jlove@mail.sdsu.edu. Phone: 619-594-2063. Fax: 619-594-4634.

Funding

This work was supported by the National Science Foundation under Career Grant No. 0448670 and the California Metabolic Research Foundation. Any opinions, findings, and conclusions or recommendations expressed in this material are those of the author(s) and do not necessarily reflect the views of the National Science Foundation. M.N. was a recipient of an Arne N. Wick Predoctoral Research Fellowship from the California Metabolic Research Foundation and of Consejo Nacional de Ciencia y Tecnologia, Mexico.

Notes

The authors declare no competing financial interest.

■ ACKNOWLEDGMENTS

We thank Professor Deborah C. Tahmassebi and Professor Tammy Dwyer of the Chemistry and Biochemistry Department at the University of San Diego for the use of their circular dichroism spectropolarimeter.

■ ABBREVIATIONS:

DUBs, deubiquitinases; UCH-L3, ubiquitin C-terminal hydrolase-L3; Ub, ubiquitin; T_m, melting (denaturation) temperature; UPS, ubiquitin-proteasome system; $t_{1/2}$, 50 percent hydrolysis point

■ REFERENCES

(1) Polo, S. (2012) Signaling-mediated control of ubiquitin ligases in endocytosis. *BMC Biol. 10*, 25.

(2) Leung, A., Geng, F., Daulny, A., Collins, G., Guzzardo, P., and Tansey, W. P. (2008) Transcriptional control and the ubiquitin-proteasome system. *Ernst Schering Found. Symp. Proc.*, 75−97.

(3) Komander, D., and Rape, M. (2012) The ubiquitin code. *Annu. Rev. Biochem. 81*, 203−229.

(4) Geng, F., Wenzel, S., and Tansey, W. P. (2012) Ubiquitin and proteasomes in transcription. *Annu. Rev. Biochem. 81*, 177−201.

(5) MacGurn, J. A., Hsu, P. C., and Emr, S. D. (2012) Ubiquitin and membrane protein turnover: from cradle to grave. *Annu. Rev. Biochem. 81*, 231−259.

(6) Xu, L., and Qu, Z. (2012) Roles of protein ubiquitination and degradation kinetics in biological oscillations. *PLoS One 7*, e34616.

(7) Hershko, A., and Ciechanover, A. (1986) The ubiquitin pathway for the degradation of intracellular proteins. *Prog. Nucleic Acid Res. Mol. Biol. 33* (19−56), 301.

(8) Behrends, C., and Harper, J. W. (2011) Constructing and decoding unconventional ubiquitin chains. *Nat. Struct. Molecular Biol. 18*, 520−528.

(9) Kulathu, Y., and Komander, D. (2012) Atypical ubiquitylation - the unexplored world of polyubiquitin beyond Lys48 and Lys63 linkages. *Nat. Rev. Mol. Cell Biol. 13*, 508−523.
(10) Keusekotten, K., Elliott, P. R., Glockner, L., Fiil, B. K., Damgaard, R. B., Kulathu, Y., Wauer, T., Hospenthal, M. K., Gyrd-Hansen, M., Krappmann, D., Hofmann, K., and Komander, D. (2013) OTULIN antagonizes LUBAC signaling by specifically hydrolyzing Met1-linked polyubiquitin. *Cell 153*, 1312−1326.
(11) Jackson, S. E. (2006) Ubiquitin: a small protein folding paradigm. *Org. Biomol. Chem. 4*, 1845−1853.
(12) Vijay-Kumar, S., Bugg, C. E., and Cook, W. J. (1987) Structure of ubiquitin refined at 1.8 Å resolution. *J. Mol. Biol. 194*, 531−544.
(13) Hagai, T., and Levy, Y. (2010) Ubiquitin not only serves as a tag but also assists degradation by inducing protein unfolding. *Proc. Natl. Acad. Sci. U S A 107*, 2001−2006.
(14) Datta, A. B., Hura, G. L., and Wolberger, C. (2009) The structure and conformation of Lys63-linked tetraubiquitin. *J. Mol. Biol. 392*, 1117−1124.
(15) Eddins, M. J., Varadan, R., Fushman, D., Pickart, C. M., and Wolberger, C. (2007) Crystal structure and solution NMR studies of Lys48-linked tetraubiquitin at neutral pH. *J. Mol. Biol. 367*, 204−211.
(16) Varadan, R., Assfalg, M., Haririnia, A., Raasi, S., Pickart, C., and Fushman, D. (2004) Solution conformation of Lys63-linked di-ubiquitin chain provides clues to functional diversity of polyubiquitin signaling. *J. Biol. Chem. 279*, 7055−7063.
(17) Komander, D. (2009) The emerging complexity of protein ubiquitination. *Biochem. Soc. Trans. 37*, 937−953.
(18) Komander, D., Reyes-Turcu, F., Licchesi, J. D., Odenwaelder, P., Wilkinson, K. D., and Barford, D. (2009) Molecular discrimination of structurally equivalent Lys 63-linked and linear polyubiquitin chains. *EMBO Reports 10*, 466−473.
(19) Hagai, T., Azia, A., Toth-Petroczy, A., and Levy, Y. (2011) Intrinsic disorder in ubiquitination substrates. *J. Mol. Biol. 412*, 319−324.
(20) Chen, X., Lee, B. H., Finley, D., and Walters, K. J. (2010) Structure of proteasome ubiquitin receptor hRpn13 and its activation by the scaffolding protein hRpn2. *Mol. Cell 38*, 404−415.
(21) Larsen, C. N., Krantz, B. A., and Wilkinson, K. D. (1998) Substrate specificity of deubiquitinating enzymes: ubiquitin C-terminal hydrolases. *Biochemistry 37*, 3358−3368.
(22) Larsen, C. N., Price, J. S., and Wilkinson, K. D. (1996) Substrate binding and catalysis by ubiquitin C-terminal hydrolases: identification of two active site residues. *Biochemistry 35*, 6735−6744.
(23) Mayer, A. N., and Wilkinson, K. D. (1989) Detection, resolution, and nomenclature of multiple ubiquitin carboxyl-terminal esterases from bovine calf thymus. *Biochemistry 28*, 166−172.
(24) Kim, J. Y., Lee, J. M., and Cho, J. Y. (2011) Ubiquitin C-terminal hydrolase-L3 regulates Smad1 ubiquitination and osteoblast differentiation. *FEBS Lett. 585*, 1121−1126.
(25) Dennissen, F. J., Kholod, N., Hermes, D. J., Kemmerling, N., Steinbusch, H. W., Dantuma, N. P., and van Leeuwen, F. W. (2011) Mutant ubiquitin (UBB+1) associated with neurodegenerative disorders is hydrolyzed by ubiquitin C-terminal hydrolase L3 (UCH-L3). *FEBS Lett. 585*, 2568−2574.
(26) Setsuie, R., Suzuki, M., Kabuta, T., Fujita, H., Miura, S., Ichihara, N., Yamada, D., Wang, Y. L., Ezaki, O., Suzuki, Y., and Wada, K. (2009) Ubiquitin C-terminal hydrolase-L3-knockout mice are resistant to diet-induced obesity and show increased activation of AMP-activated protein kinase in skeletal muscle. *FASEB J. 23*, 4148−4157.
(27) Suzuki, M., Setsuie, R., and Wada, K. (2009) Ubiquitin carboxyl-terminal hydrolase l3 promotes insulin signaling and adipogenesis. *Endocrinology 150*, 5230−5239.
(28) Setsuie, R., Suzuki, M., Tsuchiya, Y., and Wada, K. (2010) Skeletal muscles of Uchl3 knockout mice show polyubiquitinated protein accumulation and stress responses. *Neurochem. Int. 56*, 911−918.
(29) Butterworth, M. B., Edinger, R. S., Ovaa, H., Burg, D., Johnson, J. P., and Frizzell, R. A. (2007) The deubiquitinating enzyme UCH-L3 regulates the apical membrane recycling of the epithelial sodium channel. *J. Biol. Chem. 282*, 37885−37893.
(30) Fang, Y., Fu, D., and Shen, X. Z. (2010) The potential role of ubiquitin c-terminal hydrolases in oncogenesis. *Biochim. Biophys. Acta 1806*, 1−6.
(31) Issaenko, O. A., and Amerik, A. Y. (2012) Chalcone-based small-molecule inhibitors attenuate malignant phenotype via targeting deubiquitinating enzymes. *Cell Cycle 11*, 1804−1817.
(32) Nam, M. J., Madoz-Gurpide, J., Wang, H., Lescure, P., Schmalbach, C. E., Zhao, R., Misek, D. E., Kuick, R., Brenner, D. E., and Hanash, S. M. (2003) Molecular profiling of the immune response in colon cancer using protein microarrays: occurrence of autoantibodies to ubiquitin C-terminal hydrolase L3. *Proteomics 3*, 2108−2115.
(33) Rolen, U., Kobzeva, V., Gasparjan, N., Ovaa, H., Winberg, G., Kisseljov, F., and Masucci, M. G. (2006) Activity profiling of deubiquitinating enzymes in cervical carcinoma biopsies and cell lines. *Mol. Carcinog. 45*, 260−269.
(34) Misaghi, S., Galardy, P. J., Meester, W. J., Ovaa, H., Ploegh, H. L., and Gaudet, R. (2005) Structure of the ubiquitin hydrolase UCH-L3 complexed with a suicide substrate. *J. Biol. Chem. 280*, 1512−1520.
(35) Johnston, S. C., Larsen, C. N., Cook, W. J., Wilkinson, K. D., and Hill, C. P. (1997) Crystal structure of a deubiquitinating enzyme (human UCH-L3) at 1.8 A resolution. *EMBO J. 16*, 3787−3796.
(36) Lo, Y. C., Lin, S. C., Rospigliosi, C. C., Conze, D. B., Wu, C. J., Ashwell, J. D., Eliezer, D., and Wu, H. (2009) Structural basis for recognition of diubiquitins by NEMO. *Mol. Cell 33*, 602−615.
(37) Wu, C. J., Conze, D. B., Li, T., Srinivasula, S. M., and Ashwell, J. D. (2006) Sensing of Lys 63-linked polyubiquitination by NEMO is a key event in NF-kappaB activation [corrected]. *Nat. Cell Biol. 8*, 398−406.
(38) Rahighi, S., Ikeda, F., Kawasaki, M., Akutsu, M., Suzuki, N., Kato, R., Kensche, T., Uejima, T., Bloor, S., Komander, D., Randow, F., Wakatsuki, S., and Dikic, I. (2009) Specific recognition of linear ubiquitin chains by NEMO is important for NF-kappaB activation. *Cell 136*, 1098−1109.
(39) Love, J. J., Li, X., Chung, J., Dyson, H. J., and Wright, P. E. (2004) The LEF-1 high-mobility group domain undergoes a disorder-to-order transition upon formation of a complex with cognate DNA. *Biochemistry 43*, 8725−8734.
(40) Love, J. J., Li, X., Case, D. A., Giese, K., Grosschedl, R., and Wright, P. E. (1995) Structural basis for DNA bending by the architectural transcription factor LEF-1. *Nature 376*, 791−795.
(41) Barakat, N. H., Carmody, L. J., and Love, J. J. (2007) Exploiting elements of transcriptional machinery to enhance protein stability. *J. Mol. Biol. 366*, 103−116.
(42) Alexander, P. A., Rozak, D. A., Orban, J., and Bryan, P. N. (2005) Directed evolution of highly homologous proteins with different folds by phage display: implications for the protein folding code. *Biochemistry 44*, 14045−14054.
(43) Ibarra-Molero, B., Makhatadze, G. I., and Sanchez-Ruiz, J. M. (1999) Cold denaturation of ubiquitin. *Biochim. Biophys. Acta 1429*, 384−390.
(44) Wintrode, P. L., Makhatadze, G. I., and Privalov, P. L. (1994) Thermodynamics of ubiquitin unfolding. *Proteins 18*, 246−253.
(45) Huang, P. S., Love, J. J., and Mayo, S. L. (2007) A de novo designed protein protein interface. *Protein Sci. 16*, 2770−2774.
(46) Shukla, U. J., Marino, H., Huang, P., Mayo, S. L., and Love, J. J. (2004) A Designed Protein Interface that Blocks Fibril Formation. *J. Am. Chem. Soc. 126*, 13914−13915.
(47) Alexander, P., Fahnestock, S., Lee, T., Orban, J., and Bryan, P. (1992) Thermodynamic analysis of the folding of the streptococcal protein G IgG-binding domains B1 and B2: why small proteins tend to have high denaturation temperatures. *Biochemistry 31*, 3597−3603.
(48) Larsen, C. N., Krantz, B. A., and Wilkinson, K. D. (1998) Substrate specificity of deubiquitinating enzymes: ubiquitin C-terminal hydrolases. *Biochemistry 37*, 3358−68.
(49) Komander, D., Reyes-Turcu, F., Licchesi, J. D., Odenwaelder, P., Wilkinson, K. D., and Barford, D. (2009) Molecular discrimination of

structurally equivalent Lys 63-linked and linear polyubiquitin chains. *EMBO Rep 10*, 466−73.
(50) Setsuie, R., Sakurai, M., Sakaguchi, Y., and Wada, K. (2009) Ubiquitin dimers control the hydrolase activity of UCH-L3. *Neurochem. Int. 54*, 314−321.
(51) Lee, E. K., Hwang, J. H., Shin, D. Y., Kim, D. I., and Yoo, Y. J. (2005) Production of recombinant amyloid-beta peptide 42 as an ubiquitin extension. *Protein Expression Purif. 40*, 183−189.
(52) Catanzariti, A. M., Soboleva, T. A., Jans, D. A., Board, P. G., and Baker, R. T. (2004) An efficient system for high-level expression and easy purification of authentic recombinant proteins. *Protein Sci. 13*, 1331−1339.
(53) Baker, R. T., Catanzariti, A. M., Karunasekara, Y., Soboleva, T. A., Sharwood, R., Whitney, S., and Board, P. G. (2005) Using deubiquitylating enzymes as research tools. *Methods Enzymol. 398*, 540−554.
(54) Baker, R. T. (1996) Protein expression using ubiquitin fusion and cleavage. *Curr. Opin. Biotechnol. 7*, 541−546.
(55) Malakhov, M. P., Mattern, M. R., Malakhova, O. A., Drinker, M., Weeks, S. D., and Butt, T. R. (2004) SUMO fusions and SUMO-specific protease for efficient expression and purification of proteins. *Journal of Structural and Functional Genomics 5*, 75−86.
(56) Pilon, A., Yost, P., Chase, T. E., Lohnas, G., Burkett, T., Roberts, S., and Bentley, W. E. (1997) Ubiquitin fusion technology: bioprocessing of peptides. *Biotechnol. Prog. 13*, 374−379.
(57) Varshavsky, A. (2005) Ubiquitin fusion technique and related methods. *Methods Enzymol. 399*, 777−799.
(58) Patel, M. M., Sgourakis, N. G., Garcia, A. E., and Makhatadze, G. I. (2010) Experimental test of the thermodynamic model of protein cooperativity using temperature-induced unfolding of a Ubq-UIM fusion protein. *Biochemistry 49*, 8455−8467.
(59) Hicke, L., Schubert, H. L., and Hill, C. P. (2005) Ubiquitin-binding domains. *Nat. Rev. Mol. Cell Biol. 6*, 610−621.
(60) Hurley, J. H., Lee, S., and Prag, G. (2006) Ubiquitin-binding domains. *Biochem. J. 399*, 361−372.
(61) Randles, L., and Walters, K. J. (2012) Ubiquitin and its binding domains. *Front. Biosci. 17*, 2140−2157.
(62) Ye, Y., Blaser, G., Horrocks, M. H., Ruedas-Rama, M. J., Ibrahim, S., Zhukov, A. A., Orte, A., Klenerman, D., Jackson, S. E., and Komander, D. (2012) Ubiquitin chain conformation regulates recognition and activity of interacting proteins. *Nature 492*, 266−270.
(63) Enkhbayar, P., Hikichi, K., Osaki, M., Kretsinger, R. H., and Matsushima, N. (2006) 3(10)-helices in proteins are parahelices. *Proteins 64*, 691−699.
(64) Lange, O. F., Lakomek, N. A., Fares, C., Schroder, G. F., Walter, K. F., Becker, S., Meiler, J., Grubmuller, H., Griesinger, C., and de Groot, B. L. (2008) Recognition dynamics up to microseconds revealed from an RDC-derived ubiquitin ensemble in solution. *Science 320*, 1471−1475.
(65) Lakomek, N. A., Lange, O. F., Walter, K. F., Fares, C., Egger, D., Lunkenheimer, P., Meiler, J., Grubmuller, H., Becker, S., de Groot, B. L., and Griesinger, C. (2008) Residual dipolar couplings as a tool to study molecular recognition of ubiquitin. *Biochem. Soc. Trans. 36*, 1433−1437.
(66) Arviv, O., and Levy, Y. (2012) Folding of multidomain proteins: Biophysical consequences of tethering even in apparently independent folding. *Proteins 80*, 2780−2798.
(67) Yun, H. K., and Stites, W. E. (2008) Effects of Excluded Volume upon Protein Stability in Covelently Cross-Linked Proteins with Variable Linker Lengths. *Biochemistry 47*, 8804−8814.
(68) Chan, Y. L., Suzuki, K., and Wool, I. G. (1995) The carboxyl extensions of two rat ubiquitin fusion proteins are ribosomal proteins S27a and L40. *Biochem. Biophys. Res. Commun. 215*, 682−690.